AIMS Mathematics, 10(11): 27608–27634.
DOI: 10.3934/math.20251214
Received: 31 August 2025
Revised: 18 October 2025
Accepted: 28 October 2025
Published: 26 November 2025

https://www.aimspress.com/journal/Math

Research article

Dynamic behavior and bifurcation analysis of a Cournot duopoly model with log-linear price function and quadratic cost functions

Bashir Al-Hdaibat[1,*] **and A. Alameer**[2]

[1] Department of Mathematics, Faculty of Science, The Hashemite University, Zarqa, Jordan
[2] Department of Mathematics, University of Hafr Al-Batin, Hafr Al-Batin 31991, Saudi Arabia

* **Correspondence:** Email: b.alhdaibat@hu.edu.jo.

Abstract: In this paper, we studied the dynamic behavior of a Cournot-type duopoly model with homogeneous goods, a convex log-linear price function, and quadratic cost functions. By using the Lambert W function, we derived explicit expressions for the fixed points and showed that the model has exactly three fixed points. We conducted a local stability analysis to identify the stability regions for each fixed point. Furthermore, we demonstrated that the system undergoes a sequence of period-doubling bifurcations, which give rise to stable cycles of period 2 and period 4. We showed that the period-4 cycle loses its stability through a Neimark-Sacker bifurcation, where an attracting invariant closed curve emerges. We also derived the topological normal forms associated with the period-doubling bifurcation points. To confirm the presence of chaotic behavior, we computed the largest Lyapunov exponents. Finally, numerical simulations, along with bifurcation analyses performed using MatContM, validated our theoretical results. These findings extend and enhance previous studies in the literature, particularly the results in [1, 2].

Keywords: duopoly model; nonlinear dynamics; stability analysis; bifurcations; chaos; MatContM
Mathematics Subject Classification: 39A10, 39A28, 65P20, 65P30, 97N80

1. Introduction

Over the past two decades, extensive research has analyzed the complex dynamic behaviors arising in oligopolistic market models under both quantity and price competition. Oligopoly represents a market structure between the extremes of perfect competition and monopoly, as discussed in [3–5]. In an oligopolistic setting, firms exert significant but incomplete influence on market prices. Unlike in perfect competition or monopoly, firms in an oligopoly must consider not only their own production decisions but also the reactions of competing firms, adding an additional layer of complexity to market interactions.

The first mathematical model of duopoly competition was introduced by Cournot [6], describing an oligopoly with two firms competing based on output quantity. In this model, firms produce homogeneous goods, meaning consumers cannot differentiate between products. Consequently, the price of the goods is determined entirely by the total quantity produced and the market demand function. Firms adjust their production levels strategically to maximize profits. An alternative approach was proposed by Bertrand [7], in which firms compete by setting prices rather than quantities. Models based on quantity competition are referred to as Cournot-type models, while those based on price competition are known as Bertrand-type models. Together, these models form the foundation of modern oligopoly theory.

Puu [8] analyzed a Cournot duopoly model with a nonlinear demand function, revealing the presence of complex dynamics, including chaos and bifurcations. Kopel [9] examined the dynamics of Cournot duopoly models with nonlinear demand functions. Bischi and Naimzada [10] conducted a global analysis of a dynamic duopoly game with bounded rationality. Bischi and Kopel [11] explored equilibrium selection in a nonlinear duopoly game with adaptive expectations. Agiza et al. [12] investigated the complex dynamics and synchronization of duopoly games with bounded rationality. Agiza and Elsadany [13] studied the nonlinear dynamics in the Cournot duopoly game with heterogeneous players. Agliari et al. [14] examined global bifurcations related to the appearance of closed invariant curves in a Cournot duopoly model. Agliari et al. [15] analyzed global bifurcations in duopoly when the Cournot point is destabilized via a Neimark-Sacker bifurcation. Naimzada and Sbragia [16] conducted a dynamic analysis of oligopoly games with nonlinear demand and cost functions, specifically examining the stability and bifurcations of fixed points under bounded rationality. They explored how small changes in parameters can lead to significant shifts in the system's dynamics, potentially resulting in chaotic behaviors. Elettreby and Hassan [17] analyzed the dynamics of multi-team Cournot games, focusing on the stability of fixed points and the onset of bifurcations. They examined the global and local behavior of the system, exploring how interactions between multiple teams can lead to complex patterns, including periodic and chaotic dynamics, depending on the game's parameters. Ahmed, Elettreby, and Hegazi [18] extended Puu's incomplete information formulation to the multi-team Bertrand game. They provided a stability analysis of the fixed points and investigated how the introduction of incomplete information can lead to bifurcations and chaos, resulting in unpredictable competitive behaviors in the game. Naimzada and Tramontana [19] focused on controlling chaos in oligopoly games using local feedback methods. They conducted a bifurcation analysis to identify the parameters that trigger chaotic dynamics and used local control strategies to stabilize the system near its fixed points, demonstrating how local adjustments can influence the global behavior of the system. Ma and Ji [20] examined the complexity of repeated game models in electric power triopolies, analyzing the dynamic behavior of firms over repeated interactions. They investigated how the stability of fixed points and bifurcations of the system lead to chaotic dynamics, particularly in the context of asymmetric power distributions and strategic interactions between firms. Angelini, Dieci, and Nardini [21] performed a bifurcation analysis of a dynamic duopoly model with heterogeneous costs and behavioral rules. They studied how changes in these parameters affect the stability of fixed points and the system's transition from stable to chaotic behavior, providing insights into the global dynamics of oligopoly markets. Tramontana [22] continued to explore the dynamics of nonlinear duopoly models. Dubiel-Teleszynski [23] analyzed a heterogeneous duopoly game with adjusting players and

diseconomies of scale, focusing on the nonlinear dynamics and the stability of the fixed points. The study revealed that such games exhibit bifurcations that lead to chaos, and the interplay between diseconomies of scale and player adjustments influences the global dynamics of the system. Askar [24] analyzed the complex dynamic properties of Cournot duopoly games with convex and log-concave demand functions. Askar [25] explored how demand functions without inflection points contribute to the emergence of complex dynamic behaviors in Cournot duopoly games. He identified the conditions under which the system undergoes bifurcations, leading to chaotic dynamics and instability in fixed points. Sirghi, Neamțu, and Strain [26] analyzed the dynamics of a Cournot duopoly game with distributed time delays. They examined the effect of time delays on the stability of fixed points and the occurrence of bifurcations. Their study revealed that time delays could lead to periodic and chaotic dynamics, affecting the global stability of the system.

Sarafopoulos [1] investigated the complexity of a duopoly game with homogeneous goods, a convex log-linear price function, and quadratic cost functions. However, Sarafopoulos [1] did not provide a closed-form expression for the fixed points, nor did he derive the normal form for period-doubling bifurcations or discuss the existence of period-2 and higher-period cycles. The present study aims to build upon and extend the partial results of Sarafopoulos [1], offering a comprehensive analysis of the model's dynamic behavior. This includes a detailed examination of fixed points, bifurcations, period-2 and higher-period cycles, as well as chaotic dynamics. In contrast, Al-Hdaibat [2] studied the complex dynamics of the same model (such as bifurcations, periodic orbits, and chaos) with a fixed set of model parameters, varying only the speed of adjustment.

Several other studies have explored the bifurcation and chaotic behaviors in Cournot game models, offering valuable insights into the nonlinear dynamics of oligopolistic competition. These works enhance our understanding of strategic interactions and the complex dynamics in oligopolistic markets. Recent research has focused on extending and generalizing these classical models to capture more nuanced aspects of competitive behavior. Askar and Al-khedhairi [27] studied various models of Cournot duopoly games, analyzing the stability of fixed points and the occurrence of bifurcations. They found that depending on the game's parameters, the system could exhibit periodic, chaotic, or stable behaviors, and they also examined the local dynamics near the fixed points. Yang et al. [28] studied a nonlinear Stackelberg duopoly game with marginal cost considerations, highlighting the intricate dynamic interactions between bounded rational players. Peng et al. [29] explored the complex dynamics of a Cournot model incorporating relative profit delegation, demonstrating chaotic behavior through bifurcation analysis. Askar and Al-khedhairi [30] further explored the dynamics of piecewise smooth nonlinear duopoly games. They identified the bifurcation points that lead to chaos and analyzed the system's global dynamics, showing that discontinuities in the model parameters could significantly impact the system's stability. Long et al. [31] examined a dynamic Cournot-Bertrand model with imperfect rationality and incomplete information, delineating the conditions under which Nash equilibrium exists. Longfei et al. [32] investigated a Stackelberg mixed duopoly game in the insurance market, analyzing stability conditions and chaotic dynamics induced by flip bifurcation. Askar [33] studied a Cournot duopoly game with firms employing bounded rationality in production updates, identifying loss of fixed-point stability through flip and Neimark-Sacker bifurcations. Additional research has extended these concepts to other economic contexts. El Amrani et al. [34] focused on the chaotic dynamics of a duopoly game among internet service providers (ISPs) with bounded rationality. Their analysis of stability and bifurcations revealed

how bounded rationality can drive the system into chaotic behavior, with significant implications for market competition and pricing strategies. Zhu et al. [35] examined a mixed duopoly model with heterogeneous products, focusing on local and global stability using bifurcation analysis and basin-of-attraction techniques. Awad et al. [36] analyzed a differentiated Bertrand duopoly model in which semi-public firms maximize a weighted combination of social welfare and profit. Their study explored complex dynamics, synchronization, and basin-of-attraction structures. Zhang et al. [37] investigated fixed-point stability in Cournot-Bertrand duopoly models, where firms, driven by fairness considerations, may incorporate delayed decision-making. They used numerical simulations to assess the impact of key parameters on long-term market dynamics. Long and Wang [38] examined the fixed-point stability of dynamic duopoly Cournot games under heterogeneous strategies, asymmetric information, and one-way R&D spillovers. Their study involved a detailed bifurcation analysis to explore the effects of these factors on the stability of fixed points and the emergence of chaotic dynamics in the system. Wei et al. [39] studied bifurcations in a Cournot duopoly model based on bounded rationality and relative profit maximization. Their findings revealed the presence of flip bifurcations, Neimark-Sacker bifurcations, and 1:2 resonance. Meskine et al. [40] discussed a duopoly model with different types of players, also noting that the system can become chaotic through flip and Neimark-Sacker bifurcations. Askar and Alshamrani [41] examined the dynamic behavior of a Cournot-Bertrand duopoly game with nonlinear cost structures. Ahmed et al. [42] investigated a Cournot duopoly game with bounded rational players, incorporating a leader-follower dynamic in which one firm acts as a leader while the other follows. Their analysis employed center manifold and bifurcation theory to explore period-doubling and Neimark-Sacker bifurcations at the positive fixed point. In another study, Ahmed et al. [43] analyzed a Cournot-Bertrand duopoly model with heterogeneous players, examining the existence and stability of fixed points within the system. Azioune et al. [44] explored a three-player Cournot game, finding flip and Neimark-Sacker bifurcations, and discussed methods to control the resulting chaos.

In this paper, we study the dynamic behavior of a Cournot-type model with homogeneous players, convex log-linear price functions, and quadratic cost functions. We improve upon and extend the results presented in [1, 2]. The paper is organized as follows. In Section 2, we introduce the model under consideration and review some theorems and definitions that will be useful in our analysis. Section 3 derives explicit formulas for the fixed points, demonstrating that the model has exactly three fixed points. We also establish analytical conditions for the stability and bifurcation behavior of these points. In Section 4, we investigate the occurrence of period-doubling bifurcations and derive the corresponding topological normal form. Section 5 validates our theoretical findings through numerical simulations and bifurcation analysis. Using numerical continuation methods, we compute the period-doubling bifurcation curves for the fixed points and determine the bifurcation scenarios associated with each one. We show that the model undergoes four period-doubling bifurcations, leading to the emergence of higher-period cycles and chaotic attractors. As α increases, we observe stable period-2 and period-4 cycles. The period-4 cycle loses its stability via a Neimark-Sacker bifurcation, where attracting invariant closed curves emerge. Finally, we calculate the largest Lyapunov exponent to confirm the predominance of chaotic behavior.

2. Preliminaries

We consider an oligopolistic market with two firms (players) producing homogeneous goods, denoted by $i = 1, 2$. Let $x_1(n)$ and $x_2(n)$ represent the quantities supplied by firms 1 and 2, respectively, in period $n = 0, 1, 2, \ldots$. The retail price p is determined by a log-linear inverse demand function [1], which depends on the total quantity supplied by both firms in period n, $x_1(n) + x_2(n)$. The price function is given by:

$$p = a - b \ln(x_1(n) + x_2(n)),$$

where a and b are positive constants. This price function is convex and logarithmically linear, reflecting the market's sensitivity to changes in total supply.

The cost function for each firm is quadratic in nature, given by:

$$C_i(x_i) = cx_i^2, \quad i = 1, 2,$$

where c is a positive cost parameter. The profit functions for firms 1 and 2 are expressed as:

$$\Pi_i(x_i, x_j) = \left(a - b \ln\left(x_i + x_j\right)\right) x_i - C_i(x_i), \quad i, j = 1, 2, \quad i \neq j.$$

These profit functions depend on the price, which is influenced by both firms' output levels.

The marginal profit functions for each firm are derived by:

$$\pi_i(x_i, x_j) := \frac{\partial \Pi_i(x_i, x_j)}{\partial x_i} = a - b \ln\left(x_i + x_j\right) - x_i \left(2c + \frac{b}{x_i + x_j}\right), \quad i, j = 1, 2, \quad i \neq j.$$

We assume that each firm follows a bounded rationality approach, adjusting its quantity according to the sign of its marginal profit. Specifically, a firm increases (decreases) its quantity when its marginal profit is positive (negative). This adjustment is modeled by the following discrete-time dynamical system equation:

$$\frac{x_i(n+1) - x_i(n)}{x_i(n)} = \alpha \pi_i(x_i, x_j), \quad i, j = 1, 2, \quad i \neq j,$$

where $\alpha > 0$ is a parameter representing the speed of adjustment. The system dynamics are described by the following coupled difference equations:

$$x_i(n+1) = f_i\left(x_1(n), x_2(n)\right), \quad i = 1, 2, \quad n = 0, 1, 2, \ldots, \tag{2.1}$$

where

$$f_i\left(x_1(n), x_2(n)\right) = x_i(n) + \alpha x_i(n)\, \pi_i(x_i, x_j), \quad i, j = 1, 2, \quad i \neq j.$$

This system governs the dynamics of the Cournot game between the two firms. We are particularly interested in studying how the dynamics of this system evolve as a function of the parameter α, which determines the speed of adjustment in each firm's decision-making process. The resulting system provides a basis for analyzing the competition between firms and the emergence of different dynamic behaviors, including stable fixed points, periodic cycles, and chaotic dynamics, as α varies.

System (2.1) can be written more compactly in vector form as

$$\underline{x}(n+1) = \underline{f}(\underline{x}(n)), \quad n = 0, 1, 2, \ldots, \tag{2.2}$$

where $\underline{x} = (x_1, x_2) \in \mathbb{R}^2_{++}$, and $\underline{f}(\underline{x}) = (f_1(\underline{x}), f_2(\underline{x}))$ denotes the vector-valued update function. The domain $\mathbb{R}^2_{++}$ excludes boundary cases where one or both firms produce zero output, thereby restricting the analysis to scenarios of active competition between firms.

Here, we present some known results that will be useful in our study:

Definition 1. *A point $\tilde{\underline{x}}$ is called a fixed point of System (2.2) if $\underline{f}(\tilde{\underline{x}}) = \tilde{\underline{x}}$.*

Definition 2. *A solution $\left\{\underline{x}(n)\right\}_{n=0}^{\infty}$ is said to be periodic with period t if*

$$\underline{x}(n+t) = \underline{x}(n) \quad \textit{for all} \quad n \geq 0. \tag{2.3}$$

A solution $\left\{\underline{x}(n)\right\}_{n=-k}^{\infty}$ is called periodic with prime period t if t is the smallest positive integer for which System (2.3) holds.

Definition 3. *Let $\tilde{\underline{x}}$ be a fixed point of System (2.2). The fixed point is classified as follows:*

i. $\tilde{\underline{x}}$ *is* stable *if for every $\varepsilon > 0$, there exists $\delta > 0$ such that for all initial conditions $\underline{x}(0) \in \mathbb{R}^2_{++}$ satisfying $|\underline{x}(0) - \tilde{\underline{x}}| < \delta$, the trajectory remains close to $\tilde{\underline{x}}$:*

$$|\underline{x}(n) - \tilde{\underline{x}}| < \varepsilon, \quad \textit{for all } n \geq 0.$$

ii. $\tilde{\underline{x}}$ *is* locally asymptotically stable *if it is stable and, in addition, there exists $\gamma > 0$ such that for all $\underline{x}(0) \in \mathbb{R}^2_{++}$ with $|\underline{x}(0) - \tilde{\underline{x}}| < \gamma$, the trajectory converges to $\tilde{\underline{x}}$:*

$$\lim_{n\to\infty} \underline{x}(n) = \tilde{\underline{x}}.$$

iii. $\tilde{\underline{x}}$ *is* unstable *if it is not stable.*

Let $A(\tilde{\underline{x}}, \alpha)$ be the Jacobian matrix evaluated at $\tilde{\underline{x}}$. Then the characteristic equation is given by

$$\lambda^2 - \mathrm{tr}(A)\lambda + \det(A) = 0, \tag{2.4}$$

where $\mathrm{tr}(A)$ and $\det(A)$ represent the trace and determinant of the Jacobian matrix $A(\tilde{\underline{x}})$, respectively.

Theorem 1. *Assume that $\tilde{\underline{x}}$ is a fixed point of System (2.2). Then, the following statements hold:*

i. $\tilde{\underline{x}}$ *is locally asymptotically stable if all roots of the characteristic equation (2.4) (i.e., the eigenvalues) have absolute values less than 1.*
ii. $\tilde{\underline{x}}$ *is unstable if at least one root of the characteristic equation (2.4) has an absolute value greater than 1.*

3. Fixed points and their stability

Theorem 2. *System* (2.2) *has exactly three fixed points, given by*

$$\underline{\tilde{x}}_1 = \left(0,\ \frac{b}{2c}W\left[\frac{2c}{b}e^{(a-b)/b}\right]\right),$$
$$\underline{\tilde{x}}_2 = \left(\frac{b}{2c}W\left[\frac{2c}{b}e^{(a-b)/b}\right],\ 0\right),$$
$$\text{and}\quad \underline{\tilde{x}}_3 = \left(\frac{b}{2c}W\left[\frac{c}{b}e^{(2a-b)/(2b)}\right],\ \frac{b}{2c}W\left[\frac{c}{b}e^{(2a-b)/(2b)}\right]\right),$$

where $W[\cdot]$ *denotes the Lambert W-function [45].*

Proof. The fixed points of System (2.2) satisfy the equations

$$x_1 = x_1 + \alpha x_1\left(a - b\ln(x_1+x_2) - x_1\left(2c + \frac{b}{x_1+x_2}\right)\right),$$
$$x_2 = x_2 + \alpha x_2\left(a - b\ln(x_1+x_2) - x_2\left(2c + \frac{b}{x_1+x_2}\right)\right),$$

which simplify to

$$\begin{cases} \alpha x_1\left(a - b\ln(x_1+x_2) - x_1\left(2c + \dfrac{b}{x_1+x_2}\right)\right) &= 0, \\ \alpha x_2\left(a - b\ln(x_1+x_2) - x_2\left(2c + \dfrac{b}{x_1+x_2}\right)\right) &= 0. \end{cases} \tag{3.1}$$

Case 1: Let $x_1 = 0$. Then we get

$$a - b\ln(x_2) - x_2\left(2c + \frac{b}{x_2}\right) = 0.$$

Rearranging,

$$\ln(x_2) = \frac{a-b}{b} - \frac{2c}{b}x_2,$$

which implies

$$x_2 e^{(2c/b)x_2} = e^{(a-b)/b}.$$

This equation can be solved using the Lambert W-function. Therefore, we get

$$x_2 = \frac{b}{2c}W\left[\frac{2c}{b}e^{(a-b)/b}\right].$$

Thus, we obtain the first fixed point

$$\underline{\tilde{x}}_1 = \left(0, \frac{b}{2c}W\left[\frac{2c}{b}e^{(a-b)/b}\right]\right).$$

Case 2: Let $x_2 = 0$. Then by similar steps, we obtain the second fixed point

$$\underline{\tilde{x}}_2 = \left(\frac{b}{2c}W\left[\frac{2c}{b}e^{(a-b)/b}\right], 0\right).$$

Case 3: Let $x_1 \neq 0$ and $x_2 \neq 0$. If $x_1 = x_2 = \xi$, we obtain

$$a - b\ln(2\xi) - \xi\left(2c + \frac{b}{2\xi}\right) = 0.$$

Solving this equation and using the Lambert W-function, we get

$$\xi = \frac{b}{2c} W\left[\frac{c}{b} e^{(2a-b)/(2b)}\right].$$

Thus, the third fixed point is

$$\underline{\tilde{x}}_3 = \left(\frac{b}{2c} W\left[\frac{c}{b} e^{(2a-b)/(2b)}\right], \frac{b}{2c} W\left[\frac{c}{b} e^{(2a-b)/(2b)}\right]\right).$$

On the other hand, if $x_1 \neq x_2$, then System (3.1) simplifies to

$$a - b\ln(x_1 + x_2) - x_1\left(2c + \frac{b}{x_1 + x_2}\right) = 0,$$
$$a - b\ln(x_1 + x_2) - x_2\left(2c + \frac{b}{x_1 + x_2}\right) = 0.$$

Subtracting the equations gives the following equations:

$$(x_1 - x_2)\,(a - b\ln(x_1 + x_2)) = 0, \tag{3.2a}$$

$$(x_1 - x_2)\left(2c + \frac{b}{x_1 + x_2}\right) = 0. \tag{3.2b}$$

From Eq (3.2a), we get

$$a - b\ln(x_1 + x_2) = 0,$$

which implies

$$x_1 + x_2 = e^{a/b}.$$

Substituting this into Eq (3.2b), we get

$$2c + \frac{b}{e^{a/b}} = 0,$$

which leads to a contradiction since $2c + \dfrac{b}{e^{a/b}}$ is always positive for positive constants a, b, and c. Hence, no further fixed points exist beyond those already found. Thus, the three fixed points are confirmed. □

We note that the Lambert W function, $W(z)$, is generally multi-valued for real arguments, with two real branches: the principal branch $W_0(z)$ and the lower branch $W_{-1}(z)$, both defined for $z \in [-1/e, 0)$ (see [45]). In our Cournot model, the parameters a, b, and c represent strictly positive economic quantities, market size, demand sensitivity, and cost, respectively. Consequently, the arguments of the W function in the fixed points, $\frac{2c}{b} e^{(a-b)/b}$ and $\frac{c}{b} e^{(2a-b)/(2b)}$, are strictly positive. For positive arguments, the Lambert W function is single-valued in the real domain and defined only by the principal branch

W_0, while the lower branch W_{-1} is not defined. Therefore, the fixed points $\underline{\tilde{x}}_1$, $\underline{\tilde{x}}_2$, and $\underline{\tilde{x}}_3$ are the only admissible nonzero steady-state outputs in the positive quadrant of this market model. This confirms that no additional fixed points arise from the second real branch of the Lambert W function, and hence, the three fixed points derived above are exhaustive.

The following corollaries immediate follow from Theorem 1.

Corollary 1. *The fixed points $\underline{\tilde{x}}_1$ and $\underline{\tilde{x}}_2$ of System (2.2) are always unstable for all $\alpha > 0$.*

Proof. For the fixed points $\underline{\tilde{x}}_1$ and $\underline{\tilde{x}}_2$, the characteristic equation (2.4) has two eigenvalues given by

$$\lambda_{1,2} = 1 \pm \alpha k_1, \quad \text{where } k_1 := b\left(W\left[(2c/b)\mathrm{e}^{(a-b)/b}\right] + 1\right).$$

Since the term $k_1 > 0$, it follows that, for all $\alpha > 0$, at least one of the eigenvalues satisfies $|\lambda| > 1$. Therefore the fixed points $\underline{\tilde{x}}_1$ and $\underline{\tilde{x}}_2$ are unstable. □

The fixed points $\underline{\tilde{x}}_1$ and $\underline{\tilde{x}}_2$ are saddle points in the domain $0 < \alpha < 2/k_1$, where $\lambda_2 = 1 - \alpha k_1$ is the stable eigenvalue that crosses -1 at

$$\alpha_{c1} = 2/k_1.$$

Moreover, the fixed points $\underline{\tilde{x}}_1$ and $\underline{\tilde{x}}_2$ always possess a simple eigenvalue equal to -1 when $\alpha_{c1} = 2/k_1$ and a double eigenvalue equal to 1 when $\alpha = 0$.

Corollary 2. *If $\alpha \in (0, 4/(2k_2 - b))$, where $k_2 := b\left(W\left[(c/b)e^{(2a-b)/(2b)}\right] + 1\right)$, then the fixed point $\underline{\tilde{x}}_3$ of System (2.2) is locally asymptotically stable.*

Proof. For the fixed point $\underline{\tilde{x}}_3$, the characteristic equation (2.4) yields the following eigenvalues:

$$\lambda_1 = 1 - \alpha k_2, \quad \lambda_2 = 1 - \alpha(k_2 - 0.5b).$$

According to Theorem 1, the fixed point $\underline{\tilde{x}}_3$ is locally asymptotically stable if the eigenvalues satisfy $|\lambda_{1,2}| < 1$. This implies $-1 < 1 - \alpha k_2 < 1$ and $-1 < 1 - \alpha\,(k_2 - 0.5b) < 1$, and therefore

$$0 < \alpha < \min\left(\frac{2}{k_2}, \frac{2}{k_2 - 0.5b}\right).$$

Thus, the condition $|\lambda_{1,2}| < 1$ is satisfied whenever $\alpha \in \left(0, \frac{4}{2k_2 - b}\right)$. Hence, the fixed point $\underline{\tilde{x}}_3$ is locally asymptotically stable in this interval; otherwise, it is unstable. □

Note that the fixed point $\underline{\tilde{x}}_3$ always has a simple eigenvalue equal to -1 when

$$\alpha_{c2} = 2/k_2 \quad \text{and} \quad \alpha_{c3} = 4/(2k_2 - b).$$

Furthermore, it has a double eigenvalue equal to 1 when $\alpha = 0$.

The following proposition describes the period-doubling (PD) bifurcations. This type of bifurcation is important because it indicates the presence of solutions with higher periods, which can eventually lead to chaotic behavior.

Proposition 1. *System* (2.2) *undergoes four PD bifurcations at critical values of the parameter α. Specifically, the fixed points $\underline{\tilde{x}}_1$ and $\underline{\tilde{x}}_2$ undergo PD_1 and PD_2 bifurcations, respectively, when $\alpha = \alpha_{c1}$. Furthermore, the fixed point $\underline{\tilde{x}}_3$ undergoes two PD bifurcations: PD_3 occurs at $\alpha = \alpha_{c2}$ and PD_4 occurs at $\alpha = \alpha_{c3}$.*

Proof. The existence of a PD bifurcation requires two primary conditions from the standard theory (see [46]) related to the linear stability change at the critical parameter value α_c.

(i) The first condition requires that, at the bifurcation point, the Jacobian matrix of the system has a simple eigenvalue $\lambda = -1$. This condition is verified above, since the fixed points $\underline{\tilde{x}}_1$, $\underline{\tilde{x}}_2$, and $\underline{\tilde{x}}_3$ each possess a simple eigenvalue $\lambda = -1$ at $\alpha = \alpha_{c1}$, α_{c2}, and α_{c3}, respectively.

(ii) The second condition, known as the transversality condition, ensures that the critical eigenvalue $\lambda = -1$ crosses the unit circle with nonzero speed as the bifurcation parameter α varies, thus guaranteeing the bifurcation's existence. Mathematically, this requires

$$\left.\frac{d\lambda}{d\alpha}\right|_{\alpha=\alpha_c} \neq 0.$$

From the explicit expressions of the eigenvalues obtained earlier,

$$\lambda_{1,2} = 1 \pm \alpha k_1, \qquad \lambda_1 = 1 - \alpha k_2, \qquad \lambda_2 = 1 - \alpha(k_2 - 0.5b),$$

we find that the derivatives with respect to α are

$$\frac{d\lambda_{1,2}}{d\alpha} = \pm k_1, \qquad \frac{d\lambda_1}{d\alpha} = -k_2, \qquad \frac{d\lambda_2}{d\alpha} = -(k_2 - 0.5b).$$

Since $k_1 > 0$, $k_2 > 0$, and $(k_2 - 0.5b) > 0$, these derivatives are all nonzero constants. Therefore, the transversality condition is satisfied in each case.

As both the critical eigenvalue and transversality conditions hold, System (2.2) undergoes four PD bifurcations at the critical values $\alpha = \alpha_{c1}$, α_{c2}, and α_{c3}, as stated. The remaining nondegeneracy condition, which determines the stability and direction of the bifurcating periodic orbit via the normal form coefficient, is verified in Section 4. □

4. Period-doubling bifurcations

As shown in the previous sections, as the parameter α of System (2.2) varies, four PD bifurcations occur. These bifurcations are investigated using the normal form theory for discrete-time dynamical systems (see [46,47]).

Assume that for some $\alpha = \alpha_c$, System (2.2) undergoes a PD bifurcation at the fixed point $\underline{\tilde{x}}$. The Taylor expansion of $f(\underline{\tilde{x}} + \underline{x})$ about $\underline{\tilde{x}}$ is given by

$$f\left(\underline{\tilde{x}} + \underline{x}\right) = \underline{\tilde{x}} + A(\underline{\tilde{x}})\,\underline{x} + \frac{1}{2}B(\underline{x}, \underline{x}) + \frac{1}{6}C(\underline{x}, \underline{x}, \underline{x}) + \cdots,$$

where the dots denote higher-order terms in $\underline{x}$. Here, $A(\underline{\tilde{x}})$ is the Jacobian matrix evaluated at $\underline{\tilde{x}}$:

$$A(\underline{\tilde{x}}) = \begin{pmatrix} A_{1,1} & A_{1,2} \\ A_{2,1} & A_{2,2} \end{pmatrix},$$

and

$$A_{1,1} = 1 + \alpha_c\left(a - b\ln(\tilde{x}_1 + \tilde{x}_2) - \tilde{x}_1\left(2c + \frac{b}{\tilde{x}_1 + \tilde{x}_2}\right)\right) + \alpha_c\tilde{x}_1\left(\frac{\tilde{x}_1 b}{(\tilde{x}_1 + \tilde{x}_2)^2} - \frac{2b}{\tilde{x}_1 + \tilde{x}_2} - 2c\right),$$

$$A_{1,2} = \alpha_c \tilde{x}_1 \left(\frac{\tilde{x}_1 b}{(\tilde{x}_1 + \tilde{x}_2)^2} - \frac{b}{\tilde{x}_1 + \tilde{x}_2} \right),$$

$$A_{2,1} = \alpha_c \tilde{x}_2 \left(\frac{\tilde{x}_2 b}{(\tilde{x}_1 + \tilde{x}_2)^2} - \frac{b}{\tilde{x}_1 + \tilde{x}_2} \right),$$

and

$$A_{2,2} = 1 + \alpha_c \left(a - b \ln(\tilde{x}_1 + \tilde{x}_2) - \tilde{x}_2 \left(2c + \frac{b}{\tilde{x}_1 + \tilde{x}_2} \right) \right) + \alpha_c \tilde{x}_2 \left(\frac{\tilde{x}_2 b}{(\tilde{x}_1 + \tilde{x}_2)^2} - \frac{2b}{\tilde{x}_1 + \tilde{x}_2} - 2c \right),$$

while $B(\underline{x}, \underline{x})$ and $C(\underline{x}, \underline{x}, \underline{x})$ are vectors in $\mathbb{R}^2$ with components defined by

$$B(\underline{u}, \underline{v}) := \begin{pmatrix} \sum\limits_{j,k=1}^{2} \dfrac{\partial^2 f_1(\underline{\tilde{x}})}{\partial \xi_j \partial \xi_k} u_j v_k \\ \sum\limits_{j,k=1}^{2} \dfrac{\partial^2 f_2(\underline{\tilde{x}})}{\partial \xi_j \partial \xi_k} u_j v_k \end{pmatrix}, \quad C(\underline{u}, \underline{v}, \underline{w}) := \begin{pmatrix} \sum\limits_{j,k,l=1}^{2} \dfrac{\partial^3 f_1(\underline{\tilde{x}})}{\partial \xi_j \partial \xi_k \partial \xi_l} u_j v_k w_l \\ \sum\limits_{j,k,l=1}^{2} \dfrac{\partial^3 f_2(\underline{\tilde{x}})}{\partial \xi_j \partial \xi_k \partial \xi_l} u_j v_k w_l \end{pmatrix},$$

for real vectors $\underline{u} = (u_1, u_2)$, $\underline{v} = (v_1, v_2)$, and $\underline{w} = (w_1, w_2)$. When the parameter α crosses the critical values α_{ci}, $i = 1, 2, 3$, corresponding to PD bifurcations, the Jacobian matrices evaluated at $\underline{\tilde{x}}_1$, $\underline{\tilde{x}}_2$, and $\underline{\tilde{x}}_3$, respectively, possess a simple eigenvalue $\lambda = -1$. Let $\underline{q}, \underline{p} \in \mathbb{R}^2$ be right eigenvectors of $A(\underline{\tilde{x}})$ and $A^{\mathrm{T}}(\underline{\tilde{x}})$, respectively, associated with $\lambda = -1$, i.e., $A\underline{q} = \lambda \underline{q}$ and $A^{\mathrm{T}}\underline{p} = \lambda \underline{p}$. These vectors can be computed by solving the following 3×3 bordered systems:

$$\begin{pmatrix} A(\underline{\tilde{x}}) + I_2 & \underline{w}_{\mathrm{bor}} \\ \underline{v}_{\mathrm{bor}}^{\mathrm{T}} & 0 \end{pmatrix} \begin{pmatrix} \underline{q} \\ s \end{pmatrix} = \begin{pmatrix} \underline{0} \\ 1 \end{pmatrix}, \tag{4.1}$$

$$\begin{pmatrix} A^{\mathrm{T}}(\underline{\tilde{x}}) + I_2 & \underline{v}_{\mathrm{bor}} \\ \underline{w}_{\mathrm{bor}}^{\mathrm{T}} & 0 \end{pmatrix} \begin{pmatrix} \underline{p} \\ s \end{pmatrix} = \begin{pmatrix} \underline{0} \\ 1 \end{pmatrix}, \tag{4.2}$$

where $\underline{0} = (0, 0)^{\mathrm{T}}$ and $s \in \mathbb{R}$ are the same in both systems.

The bordering vectors $\underline{w}_{\mathrm{bor}}, \underline{v}_{\mathrm{bor}} \in \mathbb{R}^2$ are chosen such that the matrices

$$M(\underline{\tilde{x}}) := \begin{pmatrix} A(\underline{\tilde{x}}) + I_2 & \underline{w}_{\mathrm{bor}} \\ \underline{v}_{\mathrm{bor}}^{\mathrm{T}} & 0 \end{pmatrix}, \quad M^{\mathrm{T}}(\underline{\tilde{x}}) := \begin{pmatrix} A^{\mathrm{T}}(\underline{\tilde{x}}) + I_2 & \underline{v}_{\mathrm{bor}} \\ \underline{w}_{\mathrm{bor}}^{\mathrm{T}} & 0 \end{pmatrix}$$

are nonsingular. The eigenvectors $\underline{p}$ and $\underline{q}$ are then normalized such that

$$\langle \underline{q}, \underline{q} \rangle = \langle \underline{p}, \underline{q} \rangle = 1. \tag{4.3}$$

For parameter values $\alpha = \alpha_c$, the critical normal form coefficient of the PD bifurcation is give by (see [46, 47])

$$\theta_{\underline{\tilde{x}}}(\alpha_c) = \frac{1}{6} \left\langle \underline{p}, C(\underline{q}, \underline{q}, \underline{q}) + 3B\left(\underline{q}, (I_2 - A)^{-1} B(\underline{q}, \underline{q})\right) \right\rangle. \tag{4.4}$$

4.1. Normal form computation at PD_1

For the first PD bifurcation point (PD_1), let $\alpha = \alpha_{c1}$ and choose the bordering vectors as

$$\underline{v}_{\text{bor}} = (1,\ 1)^{\text{T}}, \quad \underline{w}_{\text{bor}} = (0,\ 1)^{\text{T}}.$$

Then the matrices

$$M\left(\underline{\tilde{x}}_1\right) = \begin{pmatrix} 4 & 0 & 0 \\ 0 & 0 & 1 \\ 1 & 1 & 0 \end{pmatrix}, \quad M^{\text{T}}\left(\underline{\tilde{x}}_1\right) = \begin{pmatrix} 4 & 0 & 1 \\ 0 & 0 & 1 \\ 0 & 1 & 0 \end{pmatrix}$$

are nonsingular. Therefore, the vectors $\underline{q}$ and $\underline{p}$ satisfying Eqs (4.1) and (4.2), and normalization condition (4.3), are given by

$$\underline{q} = \begin{pmatrix} 0 \\ 1 \end{pmatrix}, \quad \underline{p} = \begin{pmatrix} 0 \\ 1 \end{pmatrix}.$$

Next, we compute the multilinear terms:

$$B(\underline{q}, \underline{q}) = \begin{pmatrix} 0 \\ \dfrac{-4c(2z_1+1)}{b(z_1+1)z_1} \end{pmatrix}, \quad C(\underline{q}, \underline{q}, \underline{q}) = \begin{pmatrix} 0 \\ \dfrac{8c^2}{b^2(z_1+1)z_1^2} \end{pmatrix}, \quad (I_2 - A)^{-1} = \begin{pmatrix} -\dfrac{1}{2} & 0 \\ 0 & \dfrac{1}{2} \end{pmatrix},$$

where

$$z_1 = W\left[\frac{2c}{b}e^{(a-b)/b}\right] > 0.$$

Thus, we compute

$$B\left(\underline{q}, (I_2 - A)^{-1} B(\underline{q}, \underline{q})\right) = \begin{pmatrix} 0 \\ \dfrac{8c^2(2z_1+1)^2}{b^2(z_1+1)^2 z_1^2} \end{pmatrix}.$$

Using Eq (4.4), the critical normal form coefficient for the first PD bifurcation is given by

$$\theta_{\underline{\tilde{x}}_1}(\alpha_{c1}) = \frac{4c^2\left(12z_1^2 + 13z_1 + 4\right)}{3\left(bz_1(z_1+1)\right)^2} > 0. \tag{4.5}$$

4.2. Normal form computation at PD_2

Similarly, we compute the normal form coefficient (4.4) for the second PD bifurcation point PD_2. For this case, let $\alpha = \alpha_{c1}$ and the bordering vectors $\underline{w}_{\text{bor}}, \underline{v}_{\text{bor}} \in \mathbb{R}^2$ are chosen as

$$\underline{v}_{\text{bor}} = \begin{pmatrix} 1 \\ 0 \end{pmatrix}, \quad \underline{w}_{\text{bor}} = \begin{pmatrix} 1 \\ 1 \end{pmatrix}.$$

Then, the bordered matrices are given by

$$M\left(\underline{\tilde{x}}_2\right) = \begin{pmatrix} 0 & 0 & 1 \\ 0 & 4 & 1 \\ 1 & 0 & 0 \end{pmatrix}, \quad M^{\text{T}}\left(\underline{\tilde{x}}_2\right) = \begin{pmatrix} 0 & 0 & 1 \\ 0 & 4 & 0 \\ 1 & 1 & 0 \end{pmatrix},$$

which are both nonsingular. Therefore, the eigenvectors $\underline{q}$ and $\underline{p}$ satisfying (4.1), (4.2), and the normalization condition (4.3) are

$$\underline{q} = \begin{pmatrix} 1 \\ 0 \end{pmatrix}, \quad \underline{p} = \begin{pmatrix} 1 \\ 0 \end{pmatrix}.$$

Using this information, the corresponding multilinear forms are computed as

$$B(\underline{q}, \underline{q}) = \begin{pmatrix} \dfrac{-4c(2z_1+1)}{b(z_1+1)z_1} \\ 0 \end{pmatrix}, \quad C(\underline{q}, \underline{q}, \underline{q}) = \begin{pmatrix} \dfrac{8c^2}{b^2(z_1+1)z_1^2} \\ 0 \end{pmatrix},$$

and

$$(I_2 - A)^{-1} = \begin{pmatrix} \dfrac{1}{2} & 0 \\ 0 & -\dfrac{1}{2} \end{pmatrix}.$$

Hence,

$$B\left(\underline{q}, (I_2 - A)^{-1} B(\underline{q}, \underline{q})\right) = \begin{pmatrix} \dfrac{8c^2(2z_1+1)^2}{b^2(z_1+1)^2 z_1^2} \\ 0 \end{pmatrix}.$$

Substituting into (4.4), the critical normal form coefficient for $\alpha = \alpha_{c1}$ is given by

$$\theta_{\underline{\tilde{x}}_2}(\alpha_{c1}) = \theta_{\underline{\tilde{x}}_1}(\alpha_{c1}). \tag{4.6}$$

4.3. Normal form computation at PD_3

Here we compute the normal form coefficient (4.4) for the third PD bifurcation point PD_3. Let $\alpha = \alpha_{c2}$. The bordering vectors $\underline{w}_{\text{bor}}$ and $\underline{v}_{\text{bor}} \in \mathbb{R}^2$ are chosen as

$$\underline{v}_{\text{bor}} = \begin{pmatrix} 1 \\ 0 \end{pmatrix}, \quad \underline{w}_{\text{bor}} = \begin{pmatrix} 1 \\ 1 \end{pmatrix}.$$

The bordered matrices are then given by

$$M\left(\underline{\tilde{x}}_3\right) = \begin{pmatrix} \dfrac{1}{2(z_2+1)} & \dfrac{-1}{2(z_2+1)} & 1 \\ \dfrac{-1}{2(z_2+1)} & \dfrac{1}{2(z_2+1)} & 1 \\ 1 & 0 & 0 \end{pmatrix}, \quad M^{\mathrm{T}}\left(\underline{\tilde{x}}_3\right) = \begin{pmatrix} \dfrac{1}{2(z_2+1)} & \dfrac{-1}{2(z_2+1)} & 1 \\ \dfrac{-1}{2(z_2+1)} & \dfrac{1}{2(z_2+1)} & 0 \\ 1 & 1 & 0 \end{pmatrix},$$

which are both nonsingular, where

$$z_2 = W\left[\frac{c}{b} \mathrm{e}^{(2a-b)/(2b)}\right] > 0.$$

The eigenvectors $\underline{q}$ and $\underline{p}$ satisfying (4.1), (4.2), and (4.3) are

$$\underline{q} = \begin{pmatrix} \dfrac{\sqrt{2}}{2} \\ \dfrac{\sqrt{2}}{2} \end{pmatrix}, \quad \underline{p} = \begin{pmatrix} \dfrac{\sqrt{2}}{2} \\ \dfrac{\sqrt{2}}{2} \end{pmatrix}.$$

The bilinear and trilinear forms are computed as follows:

$$B(\underline{q},\underline{q}) = \begin{pmatrix} \dfrac{-2c(2z_2+1)}{bz_2(z_2+1)} \\ \dfrac{-2c(2z_2+1)}{bz_2(z_2+1)} \end{pmatrix}, \quad C(\underline{q},\underline{q},\underline{q}) = \begin{pmatrix} \dfrac{2\sqrt{2}c^2}{b^2z_2^2(z_2+1)} \\ \dfrac{2\sqrt{2}c^2}{b^2z_2^2(z_2+1)} \end{pmatrix}.$$

The inverse matrix $(I_2 - A)^{-1}$ is given by

$$(I_2 - A)^{-1} = \begin{pmatrix} \dfrac{3+4z_2}{8z_2+4} & \dfrac{-1}{8z_2+4} \\ \dfrac{-1}{8z_2+4} & \dfrac{3+4z_2}{8z_2+4} \end{pmatrix}.$$

Thus,

$$B\left(\underline{q},(I_2 - A)^{-1}B(\underline{q},\underline{q})\right) = \begin{pmatrix} \dfrac{2\sqrt{2}c^2(2z_2+1)^2}{b^2z_2^2(z_2+1)^2} \\ \dfrac{2\sqrt{2}c^2(2z_2+1)^2}{b^2z_2^2(z_2+1)^2} \end{pmatrix}.$$

According to (4.4), the critical normal form coefficient for the third PD point is

$$\theta_{\underline{\tilde{x}}_3}(\alpha_{c2}) = \frac{2c^2\left(12z_2^2+13z_2+4\right)}{3\left(bz_2(z_2+1)\right)^2} > 0. \tag{4.7}$$

4.4. Normal form computation at PD_4

Similarly, we compute the normal form coefficient (4.4) for the fourth PD bifurcation point PD_4. Let $\alpha = \alpha_{c3}$, and then the bordering vectors $\underline{w}_{\text{bor}}$ and $\underline{v}_{\text{bor}} \in \mathbb{R}^2$ are chosen as

$$\underline{v}_{\text{bor}} = \begin{pmatrix} 1 \\ 0 \end{pmatrix}, \quad \underline{w}_{\text{bor}} = \begin{pmatrix} 0 \\ 1 \end{pmatrix}.$$

Then, the bordered matrices are

$$M\left(\underline{\tilde{x}}_3\right) = \begin{pmatrix} \dfrac{-1}{2z_2+1} & \dfrac{-1}{2z_2+1} & 0 \\ \dfrac{-1}{2z_2+1} & \dfrac{-1}{2z_2+1} & 1 \\ 1 & 0 & 0 \end{pmatrix}, \quad M^{\text{T}}\left(\underline{\tilde{x}}_3\right) = \begin{pmatrix} \dfrac{-1}{2z_2+1} & \dfrac{-1}{2z_2+1} & 1 \\ \dfrac{-1}{2z_2+1} & \dfrac{-1}{2z_2+1} & 0 \\ 0 & 1 & 0 \end{pmatrix},$$

which are nonsingular.

Therefore, the eigenvectors $\underline{q}$ and $\underline{p}$ satisfying (4.1), (4.2), and (4.3) are

$$\underline{q} = \begin{pmatrix} \dfrac{\sqrt{2}}{2} \\ -\dfrac{\sqrt{2}}{2} \end{pmatrix}, \quad \underline{p} = \begin{pmatrix} \dfrac{\sqrt{2}}{2} \\ -\dfrac{\sqrt{2}}{2} \end{pmatrix}.$$

The bilinear and trilinear forms are computed as follows:

$$B(\underline{q},\underline{q}) = \begin{pmatrix} \dfrac{-4c}{bz_2} \\ \dfrac{-4c}{bz_2} \end{pmatrix}, \quad C(\underline{q},\underline{q},\underline{q}) = \begin{pmatrix} 0 \\ 0 \end{pmatrix}.$$

The inverse matrix $(I_2 - A)^{-1}$ is given by

$$(I_2 - A)^{-1} = \begin{pmatrix} \dfrac{3+4z_2}{8z_2+8} & \dfrac{-1}{8z_2+8} \\ \dfrac{-1}{8z_2+8} & \dfrac{3+4z_2}{8z_2+8} \end{pmatrix}.$$

Hence,

$$B\left(\underline{q},(I_2 - A)^{-1}B(\underline{q},\underline{q})\right) = \begin{pmatrix} \dfrac{4\sqrt{2}c^2(2z_2+1)}{b^2z_2^2(z_2+1)} \\ \dfrac{-4\sqrt{2}c^2(2z_2+1)}{b^2z_2^2(z_2+1)} \end{pmatrix}.$$

For parameter value $\alpha = \alpha_{c3}$, the critical normal form coefficient is

$$\theta_{\underline{\tilde{x}}_3}(\alpha_{c3}) = \frac{4c^2(2z_2+1)}{b^2z_2^2(z_2+1)} > 0. \tag{4.8}$$

Based on the computed normal form coefficients at each *PD* point in Eqs (4.5)–(4.8), we state the following theorem.

Theorem 3. *For parameter values α close to the PD bifurcation value α_c, the restriction of System (2.2) to a parameter-dependent center manifold is locally smoothly equivalent to the topological normal form*

$$\xi \mapsto -(1+\beta(\alpha))\,\xi + \theta_{\underline{\tilde{x}}}(\alpha_c)\xi^3 + O(\xi^4), \tag{4.9}$$

where $\xi \in \mathbb{R}$ denotes the local coordinate on the center manifold near the fixed point $\underline{\tilde{x}}$, $\beta(\alpha_c) = 0$, and $\theta_{\underline{\tilde{x}}}(\alpha_c)$ is given in Eqs (4.5)–(4.8). The $O(\xi^4)$ terms may depend on α.

It is important to note that the normal form coefficient of a PD bifurcation describes the stability of the new period-2 cycle only on the center manifold. The fixed points $\underline{\tilde{x}}_{1,2}$ of System (2.2) are unstable for all $\alpha > 0$, but they act as saddle points for $\alpha \in (0, \alpha_{c1})$, possessing both stable and unstable manifolds. When the PD bifurcation occurs at $PD_{1,2}$, the new period-2 cycle inherits the transverse instability of $\underline{\tilde{x}}_{1,2}$. Its stability along the center manifold depends on the normal form coefficient; even if the normal form coefficients (4.5) and (4.6) are positive (supercritical), the cycle remains unstable in the full 2D phase space, resulting in a period-2 saddle. This mechanism repeats: unstable period-2 cycles give rise to unstable period-4 cycles, and so on. A similar conclusion can be derived for the fixed point $\underline{\tilde{x}}_4$.

In contrast, the fixed point $\underline{\tilde{x}}_3$ is stable for $\alpha \in (0, \alpha_{c2})$ and loses stability at PD_3. Since it has no unstable transverse directions before the bifurcation point, the stability of the emerging period-2 cycle is governed entirely by the bifurcation type. With a positive normal form coefficient (4.7), a supercritical bifurcation occurs, producing a stable period-2 cycle, which can further generate a stable period-4 cycle.

5. Numerical simulation

System (2.2) exhibits a symmetry property under the transformation $x_1 \leftrightarrow x_2$. As demonstrated in the previous sections, the set of fixed points and bifurcations also reflects this symmetry about the line $x_1 = x_2$. Therefore, it suffices to consider the fixed points $\underline{\tilde{x}}_2$ and $\underline{\tilde{x}}_3$ to capture the full range of bifurcation structures, periodic dynamics, attracting invariant curves, and chaotic behaviors of System (2.2).

5.1. Bifurcation diagram

We consider a bifurcation diagram generated in MATLAB for the fixed points $\underline{\tilde{x}}_2$ and $\underline{\tilde{x}}_3$ of System (2.2); see Figure 1. The diagram is obtained by fixing the parameters $a = 1$, $b = 1$, and $c = 0.5$, while varying the parameter α in the interval $[0, 2]$ with a step size of 0.001. For each value of α, the system is iterated 1000 times, and the first 100 iterations are discarded to eliminate transients.

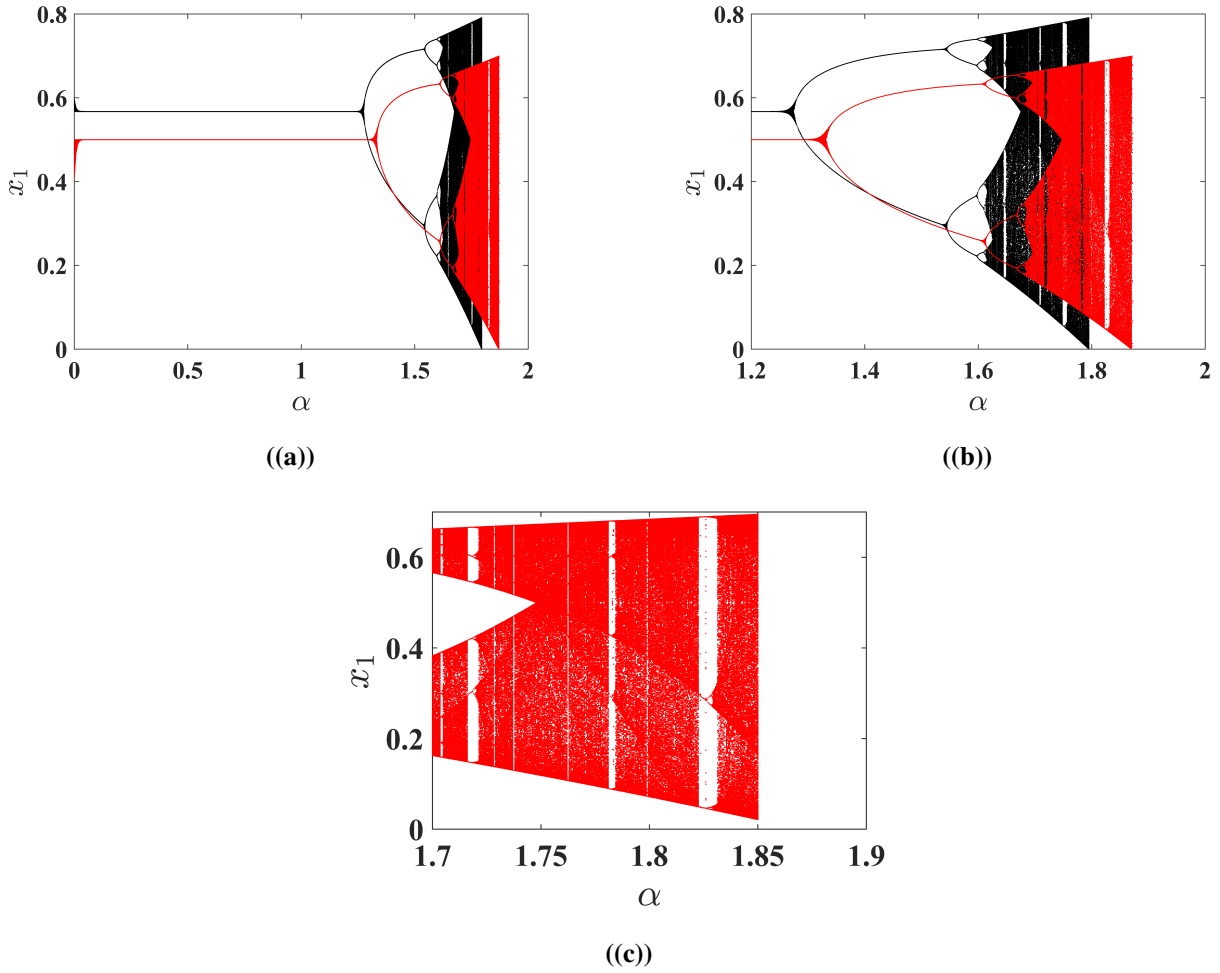

Figure 1. Bifurcation diagram of System (2.2) for the fixed points $\underline{\tilde{x}}_2$ (black curve) and $\underline{\tilde{x}}_3$ (red curve), with parameters $a = 1$, $b = 1$, and $c = 0.5$. The bifurcation parameter α varies in the intervals (a) $[0, 2]$, (b) $[1.2, 2]$, and (c) $[1.7, 1.9]$.

The bifurcation diagram of the fixed point $\underline{\tilde{x}}_2$ reveals that near the critical value $\alpha \approx 1.28$, the fixed point undergoes a PD bifurcation (corresponding to the PD_2 point), giving rise to an unstable period-2 cycle. As α increases further, a cascade of PD bifurcations emerges, eventually leading to chaotic dynamics. Within the chaotic intervals, periodic windows corresponding to higher-period cycles appear. Figure 1(b) presents a zoomed-in view of Figure 1(a), generated using the same numerical parameters. A similar dynamical behavior is exhibited by the fixed point $\underline{\tilde{x}}_3$, which undergoes a supercritical PD bifurcation at $\alpha \approx 1.3$, corresponding to the bifurcation point PD_3. Beyond this point, $\underline{\tilde{x}}_3$ loses stability, giving rise to a new, stable period-2 cycle that becomes the system's attractor. The solution then experiences successive PD bifurcations followed by transitions into chaos, interspersed with periodic cycles of various periods.

To further examine the fine structure of the chaotic region associated with $\underline{\tilde{x}}_3$, we generate a zoomed-in bifurcation diagram while varying the parameter α in the interval $[1.7, 1.9]$ with a step size of 0.0005. It is evident from this refined view that periodic windows consistently emerge within this chaotic interval; see Figure 1(c).

As a result, the entire cascade of bifurcations originating from the $\underline{\tilde{x}}_2$ branch consists of unstable cycles, a result confirmed using MatContM in the next subsection. This observation highlights an important feature of the system's dynamics: the coexistence of stable attractors. Our numerical simulations (see Figure 1) clearly show stable period-2 and period-4 attractors in the same parameter regions. These stable attractors coexist with the unstable saddle cycles that originate from $\underline{\tilde{x}}_2$. This explains why traces of the stable period-2 and period-4 attractors appear superimposed on the bifurcation diagram of the unstable $\underline{\tilde{x}}_2$ fixed point in Figure 1.

We conduct a numerical bifurcation analysis of System (2.2) using the MatContM package in MATLAB, which is based on numerical continuation methods (see [48, 49]). For this analysis, we fix the model parameters at $a = 1$, $b = 1$, and $c = 0.5$, and treat α as the bifurcation parameter.

Table 1. Detection of PD bifurcations during the continuation of fixed points of System (2.2) using MatContM.

Label	x_1	x_2	α	Normal form coefficient
PD_1	0	0.567143	1.276207	6.427648
PD_2	0.567143	0	1.276207	6.427648
PD_3	0.5	0.5	1.333333	4
PD_4	0.5	0.5	2	5.333333

Starting from the initial values $(x_1, x_2, \alpha) = (0, 0.5671433, 10^{-6})$, the continuation of the fixed-point branch leads to the detection of a PD bifurcation point, denoted as PD_1 in Table 1. This point lies on the blue branch of the bifurcation diagram shown in Figure 2, corresponding to the fixed point $\underline{\tilde{x}}_1$. Repeating the continuation with initial values $(x_1, x_2, \alpha) = (0.5671433, 0, 10^{-6})$, another PD bifurcation is detected at the same value of α. This point, labeled PD_2, is found on the red branch corresponding to the fixed point $\underline{\tilde{x}}_3$. Using the initial values $(x_1, x_2, \alpha) = (0.5, 0.5, 10^{-6})$, two additional PD bifurcation points, PD_3 and PD_4, are detected along the green branch of the bifurcation diagram, which corresponds to the fixed point $\underline{\tilde{x}}_2$. The corresponding normal form coefficients, computed using MatContM, are summarized together with all relevant results in Table 1.

A period-2 cycle arising from the PD_2 point was continued using α as the free parameter with the

initial data $(x_1, x_2, \alpha) = (0.5, 0, 1.28)$. This cycle is represented by the dashed red curve in Figure 2. Similarly, a second period-2 cycle, originating from the PD_3 point, was continued from the initial data $(x_1, x_2, \alpha) = (0.6, 0.5, 1.33333)$ and is shown as the dashed green curve in Figure 2. Further PD bifurcations were detected along both of these period-2 cycles.

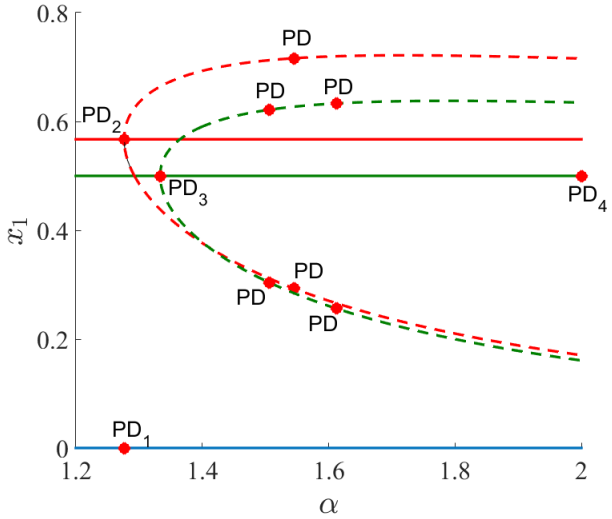

Figure 2. Bifurcation diagram of fixed points of System (2.2) computed using `MatContM`. The blue, red, and green solid branches correspond to the fixed points $\tilde{x}_1$, $\tilde{x}_3$, and $\tilde{x}_2$, respectively. The dashed curves represent the emerging period-2 cycles.

To validate the theoretical findings in Sections 3 and 4, we compute the same bifurcation data analytically for $a = 1$, $b = 1$, and $c = 0.5$. The fixed-point values x_1 and x_2 are obtained using Theorem 2, the corresponding values of α are derived from Proposition 1, and the normal form coefficients are calculated using Eqs (4.5)–(4.8). These analytical results are summarized in Table 2.

Table 2. Analytically computed bifurcation data for System (2.2) based on Theorem 2, Proposition 1, and Eqs (4.5)–(4.8).

Label	x_1	x_2	α	Normal form coefficient
PD_1	0	0.5671432904	1.276207487	6.427647899
PD_2	0.5671432904	0	1.276207487	6.427647899
PD_3	0.5	0.5	1.333333333	4
PD_4	0.5	0.5	2	5.333333330

The agreement between the numerical results in Table 1 and the analytical computations in Table 2 confirms the theoretical findings presented in Sections 3 and 4, thus validating our bifurcation analysis of System (2.2).

5.2. Periodic solutions and their stability

As illustrated in Figure 2, the system undergoes a sequence of PD bifurcations as the parameter α increases, revealing its rich underlying dynamics. We performed a numerical stability analysis for

the period-2 cycles of System (2.2). During the continuation of the period-2 cycles, we monitor the eigenvalues to determine cycle stability. The period-2 cycle arising from PD_2 is always unstable, as one of its multipliers always has a magnitude greater than 1. In contrast, the cycle arising from PD_3 is stable on the interval $\alpha \in (1.33333, 1.506082)$ but loses its stability at $\alpha \approx 1.506082$ via a subsequent PD bifurcation, as shown in Figure 3. The existence of PD bifurcations on these period-2 cycles indicates the presence of cycles of higher periods.

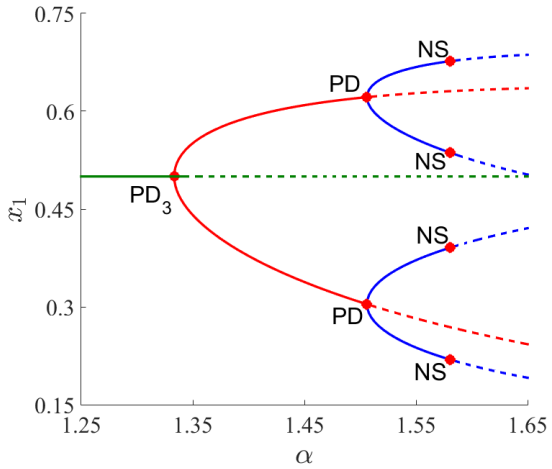

Figure 3. A stability analysis of the period-4 cycle calculated using MatContM. The period-2 cycle is shown in red and the period-4 cycle is in blue. The fixed point $\tilde{x}_3$ is also indicated in green. Solid lines represent stable solutions, while dashed lines represent unstable ones.

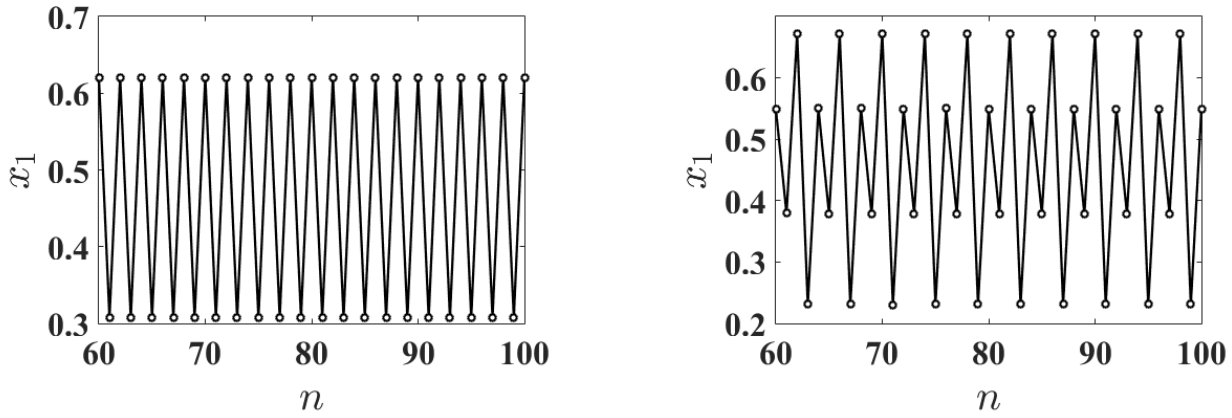

((**a**)) Period-2 cycle at $\alpha = 1.5$ ((**b**)) Period-4 cycle at $\alpha = 1.56$

Figure 4. Periodic cycles for selected values of α in System (2.2).

We then performed a numerical continuation of the period-4 cycle arising from PD_3 using MatContM with α as the free parameter. The continuation was initiated from points on the cycle at $\alpha = 1.56$, including $(x_1, x_2) = (0.3785, 0.2308)$ and $(x_1, x_2) = (0.6712, 0.5498)$. This analysis, summarized in Figure 3, revealed that the period-4 cycle is stable within the interval $\alpha \in (1.506082, 1.580383)$. The lower bound marks the PD_3 bifurcation where the cycle originates,

and the upper bound corresponds to a Neimark-Sacker (NS) bifurcation $\alpha_{NS} = 1.580383$. In Figure 3, the period-2 cycle is shown in red, the period-4 cycle in blue, and the fixed point $\underline{\tilde{x}}_3$ in green. Solid lines indicate stable solutions, while dashed lines denote unstable ones.

To observe these cycles, we fix the parameters at $a = 1$, $b = 1$, and $c = 0.5$.

- When we iterate System (2.2) with initial values $(x_1, x_2) = (0.62, 0.62)$ at $\alpha = 1.5$, we observe a stable period-2 cycle, as shown in Figure 4(a).
- By iterating the system with initial values $(x_1, x_2) = (0.65, 0.45)$ at $\alpha = 1.56$, we observe a stable period-4 cycle, as shown in Figure 4(b).

5.3. Chaotic attractors

The period-4 cycle loses its stability through the NS bifurcation at ($\alpha = \alpha_{NS}$). As determined using MatContM, the first Lyapunov exponent associated with this bifurcation is negative. This implies the bifurcation is supercritical, meaning an attracting invariant closed curve (a quasi-periodic orbit) emerges as the cycle becomes unstable.

Figure 5 illustrates this phenomenon at $\alpha = 1.5804$, just past the bifurcation point. These plots were generated for System (2.2) with parameters $a = 1$, $b = 1$, $c = 0.5$ and initial conditions $(x_1, x_2) = (0.2, 0.1)$. Figure 5(a) shows the "ghost" of the now-unstable period-4 cycle at $\alpha = 1.5804 > \alpha_{NS}$ as the trajectory settles onto the new attracting curve. Figure 5(b) provides a zoomed-in view, clearly depicting this invariant closed curve.

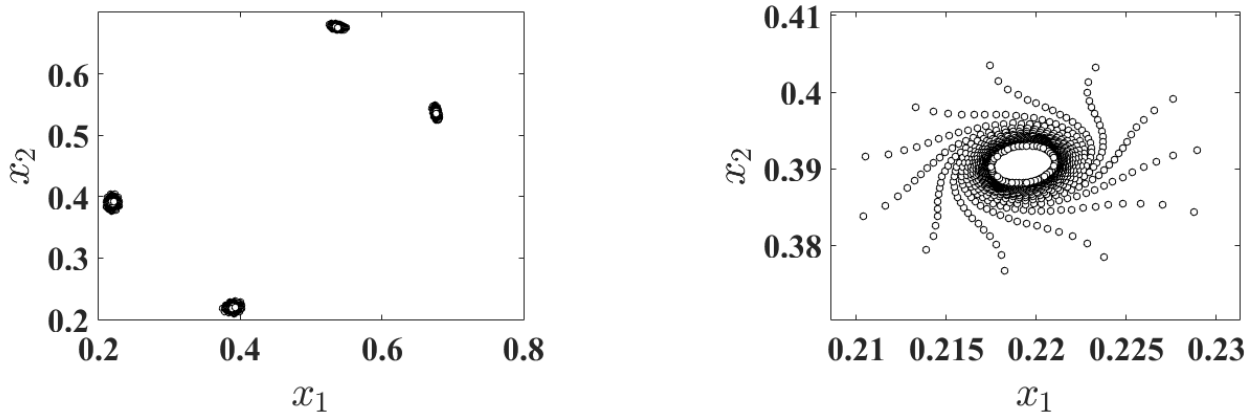

Figure 5. Emergence of an attracting invariant closed curve for System (2.2) at $\alpha = 1.5804$, immediately following the NS bifurcation.

As the parameter α exceeds approximately 1.62, the system exhibits aperiodic behavior consistent with deterministic chaos. This is evidenced by the chaotic attractors observed for $\alpha = 1.62$, $\alpha = 1.65$, and $\alpha = 1.7$, which are shown in Figures 6(a)–6(c). These attractors highlight the sensitivity to initial conditions and irregular oscillations characteristic of chaotic dynamics.

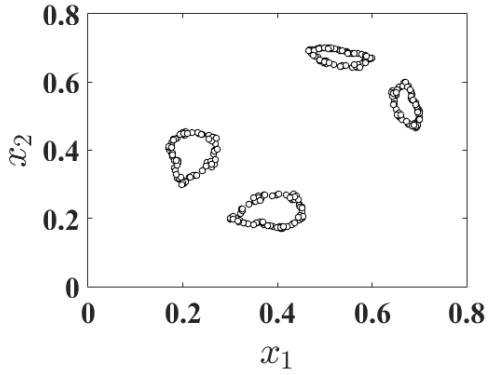

((a)) Chaotic attractor at $\alpha = 1.62$

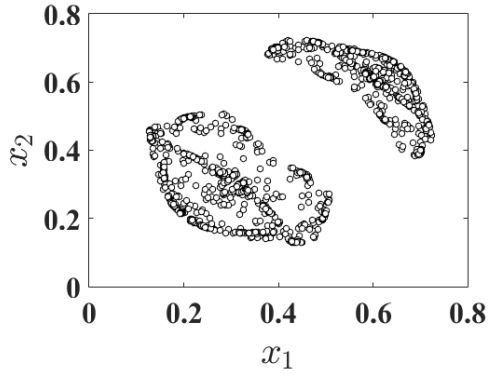

((b)) Chaotic attractor at $\alpha = 1.65$

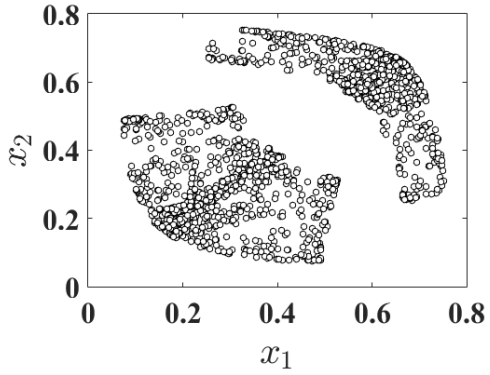

((c)) Chaotic attractor at $\alpha = 1.7$

Figure 6. Chaotic attractors observed for increasing values of $\alpha > 1.62$, indicating the transition to aperiodic and unpredictable behavior.

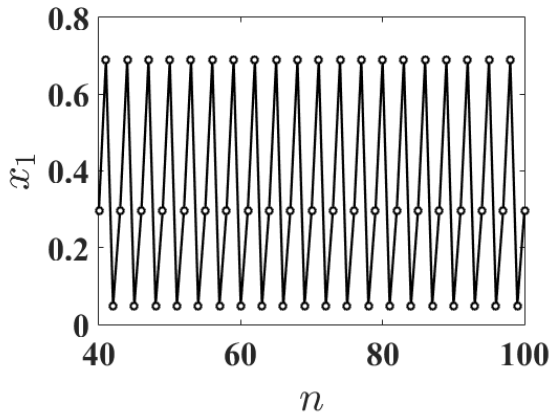

((a)) Period-3 cycle at $\alpha = 1.823$

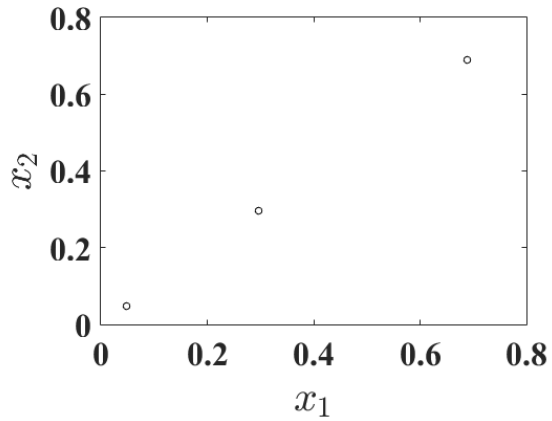

((b)) Phase plot of period-3 cycle at $\alpha = 1.823$

Figure 7. Period-3 cycle at $\alpha = 1.823$, representing a periodic window embedded within the chaotic region of System (2.2).

Interestingly, within this chaotic interval (for $\alpha > 1.61$), the system exhibits periodic windows. For instance, if we fix the parameters $a = 1$, $b = 1$, and $c = 0.5$ and iterate System (2.2) with initial values $(x_2, x_1) = (0.65, 0.65)$, a period-3 cycle emerges at $\alpha = 1.823$, as illustrated in Figures 7(a) and 7(b). This phenomenon of periodicity within chaos highlights the rich and complex dynamics of System (2.2).

To the best of our knowledge, these periodic and chaotic behaviors have not been previously reported in the context of System (2.2). The identification of these rich dynamical patterns contributes novel insights into the nonlinear dynamics of System (2.2).

5.4. Analysis by Lyapunov exponents

A key way to measure chaos in a dynamical system is the Lyapunov exponent, which measures the average exponential rate at which nearby orbits separate. A positive Lyapunov exponent provides strong evidence for chaotic dynamics.

We computed the *largest Lyapunov exponent* for System (2.2). To do this, we fixed the parameters $a = 1$, $b = 1$, and $c = 0.5$, and varied the bifurcation parameter α in the interval $[0, 2]$ with a step size of 0.0001. For each α value, the system was iterated 1000 times, and we discarded the first 100 iterations to remove any transient dynamics.

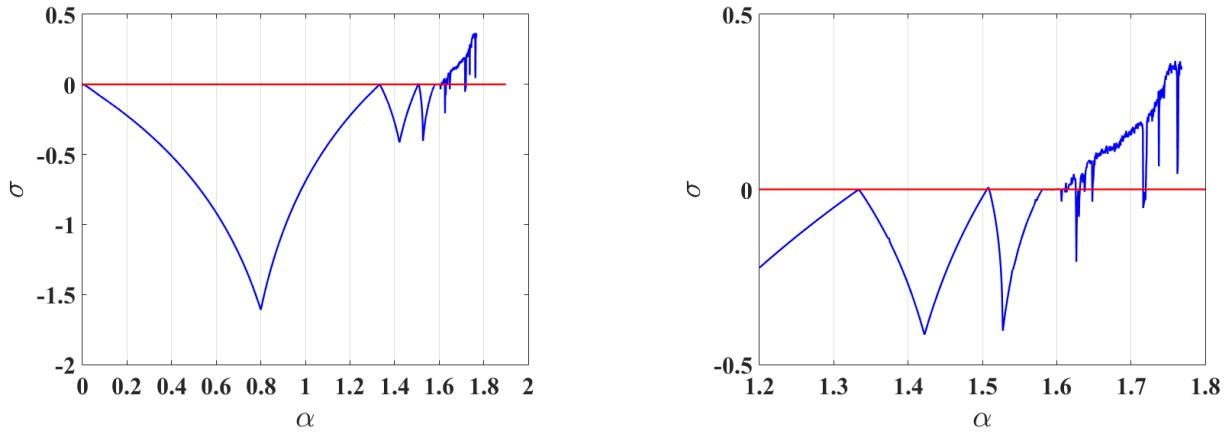

((a)) Lyapunov exponent σ for $\alpha \in [0, 2]$.

((b)) Zoomed-in view for $\alpha \in [1.2, 1.8]$.

Figure 8. Largest Lyapunov exponent σ as a function of the bifurcation parameter α. Positive values confirm the presence of chaos.

The computed Lyapunov exponents are presented in Figure 8. By comparing the exponent plot (Figure 8(a)) with the bifurcation diagram (Figure 1(a) and Figure 3), the transitions between periodic and chaotic states become much clearer.

- For $\alpha \in [0, 1.58)$, the Lyapunov exponent remains negative. This reflects the stability of the fixed point $\underline{\tilde{x}}_3$ as well as the stable period-2 and period-4 cycles.
- The exponent approaches zero near $\alpha \approx 1.33$ and $\alpha \approx 1.51$, which are the points where the stable period-2 and period-4 cycles emerge, respectively.
- As α increases further, the Lyapunov exponent oscillates between negative, zero, and positive values. This indicates alternating regions of stable periodic cycles, attracting invariant closed

curves, PD bifurcations, and chaotic behavior.

- Specifically, for $\alpha \in (1.62, 1.8)$, the Lyapunov exponent becomes strictly positive (see Figure 8(b)), confirming the presence of chaotic behavior within this interval.

6. Conclusions

In this study, we have explored the complex dynamics of a discrete-time Cournot-type duopoly model incorporating homogeneous goods, a convex log-linear price function, and quadratic cost functions. By employing analytical and numerical techniques, we have provided a comprehensive understanding of the model's qualitative behavior.

Using the Lambert W function, we obtained explicit expressions for the fixed points and showed that the system has exactly three fixed points. A local stability analysis identified the parameter intervals associated with stable behavior.

A core finding is the direct link between the speed of adjustment parameter α and market stability. Low values of α denote conservative, near-rational competitive behavior that guarantees market stability and convergence to the unique symmetric Cournot equilibrium steady state. Conversely, high values of α indicate firms exhibiting excessive aggressiveness or bounded rationality in their output decisions. This overreaction is the mechanism driving the complex dynamics.

We identified a sequence of period-doubling (PD) bifurcations leading to the onset of chaos. Cycles of period-2, period-4, attracting invariant closed curves, and chaotic attractors were observed as α increased, illustrating a classical route to chaos. This sequence represents a transition to persistent output oscillation and increasing market uncertainty, while the onset of chaos signifies a complete breakdown of predictable market dynamics, rendering output and pricing highly volatile and unpredictable.

We also derived the topological normal forms at the PD points to gain insight into the bifurcation structure and the stability of the emerging periodic orbits. To confirm the existence of chaotic dynamics, we computed the largest Lyapunov exponent. Furthermore, numerical simulations revealed the presence of periodic windows embedded within chaotic regions, including a period-3 cycle. The numerical bifurcation analysis performed using MatContM confirmed the theoretical findings. The results highlight the effectiveness of combining analytical tools with numerical continuation techniques for investigating nonlinear economic models.

To the best of our knowledge, the comprehensive bifurcation and chaos analysis presented in this work (particularly the detection of multiple period-doubling cascades, the derivation of normal form coefficients, the identification of a Neimark–Sacker bifurcation and the corresponding closed invariant curves, and the observation of periodic cycles of orders 2, 3, and 4 along with chaotic intervals) has not been previously reported for System (2.2). This study enhances our understanding of the rich dynamical behavior that can arise in System (2.2) and extends previous results in the literature [1, 2].

Future work could consider the effects of heterogeneous expectations, stochastic perturbations, or time delays on the stability and bifurcation structure of the model, further enriching the theoretical insights and practical relevance of such economic systems.

Author contributions

Bashir Al-Hdaibat: Conceptualization, formal analysis, methodology, validation, visualization, writing—original draft; A. Alameer: Conceptualization, formal analysis, methodology, validation. All authors have read and agreed to the published version of the manuscript.

Use of Generative-AI tools declaration

The authors declare that they have not used Artificial Intelligence (AI) tools in the creation of this article.

Conflict of interest

The authors declare that they have no conflicts of interest.

References

1. G. Sarafopoulos, Complexity in a duopoly game with homogeneous players, convex, log-linear demand and quadratic cost functions, *Proc. Econ. Finance*, **33** (2015), 358–366. http://doi.org/10.1016/S2212-5671(15)01720-7
2. B. Al-Hdaibat, Bifurcations in a chaotic duopoly game with a logarithmic demand function, *Dyn. Contin., Discrete Impulsive Syst. Ser. B: Appl. Algorithms*, **26** (2019), 389–407.
3. T. Puu, *Nonlinear Economic Dynamics*, Berlin: Springer-Verlag, 1997.
4. R. B. Myerson, Nash equilibrium and the history of economic theory, *J. Econ. Lit.*, **37** (1999), 1067–1082. http://doi.org/10.1257/jel.37.3.1067
5. B. Al-Hdaibat, W. Govaerts, N. Neirynck, On periodic and chaotic behavior in a two-dimensional monopoly model, *Chaos, Solitons Fractals*, **70** (2015), 27–37. http://doi.org/10.1016/j.chaos.2014.10.010
6. A. Cournot, *Recherches sur les Principes Math'ematiques de la Th'eorie des Richesses*, Hachette, 1838.
7. J. Bertrand, Théorie mathématique de la richesse sociale, In: *Cournot Oligopol*y, Cambridge University Press, 1988, 73–81.
8. T. Puu, The chaotic monopolist, *Chaos, Solitons Fractals*, **5** (1995), 35–44. http://doi.org/10.1016/0960-0779(94)00206-6
9. M. Kopel, Simple and complex adjustment dynamics in cournot duopoly models, *Chaos, Solitons Fractals*, **7** (1996), 2031–2048. http://doi.org/10.1016/S0960-0779(96)00070-7
10. G. I. Bischi, A. Naimzada, Global analysis of a dynamic duopoly game with bounded rationality, *Adv. Dyn. Games Appl.*, **5** (1999), 361–385.
11. G. I. Bischi, M. Kopel, Equilibrium selection in a nonlinear duopoly game with adaptive expectations, *J. Econ. Behav. Organ.*, **46** (2001), 73–100.

12. H. N. Agiza, A. S. Hegazi, A. A. Elsadany, Complex dynamics and synchronization of duopoly game with bounded rationality, *Math. Comput. Simul.*, **58** (2002), 133–146.

13. H. N. Agiza, A. A. Elsadany, Nonlinear dynamics in the cournot duopoly game with heterogeneous players, *Phys. A*, **320** (2003), 512–524. http://doi.org/10.1016/S0378-4371(02)01648-5

14. A. Agliari, L. Gardini, T. Puu, Some global bifurcations related to the appearance of closed invariant curves, *Math. Comput. Simul.*, **68** (2005), 201–219.

15. A. Agliari, L. Gardini, T. Puu, Global bifurcations in duopoly when the cournot point is destabilized via a subcritical neimark bifurcation, *Int. Game Theory Rev.*, **8** (2006), 1–20.

16. A. K. Naimzada, L. Sbragia, Oligopoly games with nonlinear demand and cost functions: Two boundedly rational adjustment processes, *Chaos, Solitons Fractals*, **29** (2006), 707–722. http://doi.org/10.1016/j.chaos.2005.08.103

17. M. F. Elettreby, S. Z. Hassan, Dynamical multi-team Cournot game, *Chaos, Solitons Fractals*, **27** (2006), 666–672. http://doi.org/10.1016/j.chaos.2005.04.075

18. E. Ahmed, M. F. Elettreby, A. S. Hegazi, On Puu's incomplete information formulation for the standard and multi-team Bertrand game, *Chaos, Solitons Fractals*, **30** (2006), 1180–1184. http://doi.org/10.1016/j.chaos.2005.08.198

19. A. K. Naimzada, F. Tramontana, Controlling chaos through local knowledge, *Chaos, Solitons Fractals*, **42** (2009), 2439–2449. http://doi.org/10.1016/j.chaos.2009.03.109

20. J.-H. Ma, W.-Z. Ji, Complexity of repeated game model in electric power triopoly, *Chaos, Solitons Fractals*, **40** (2009), 1735–1740. http://doi.org/10.1016/j.chaos.2007.09.058

21. N. Angelini, R. Dieci, F. Nardini, Bifurcation analysis of a dynamic duopoly model with heterogeneous costs and behavioural rules, *Math. Comput. Simul.*, **79** (2009), 3179–3196.

22. F. Tramontana, Heterogeneous duopoly with isoelastic demand function, *Econ. Modell.*, **27** (2010), 350–357. http://doi.org/10.1016/j.econmod.2009.09.014

23. T. Dubiel-Teleszynski, Nonlinear dynamics in a heterogeneous duopoly game with adjusting players and diseconomies of scale, *Commun. Nonlinear Sci. Numer. Simul.*, **16** (2011), 296–308. https://doi.org/10.1016/j.cnsns.2010.03.002

24. S. S. Askar, Complex dynamic properties of cournot duopoly games with convex and log-concave demand function, *Oper. Res. Lett.*, **42** (2014), 85–90. http://doi.org/10.1016/j.orl.2013.12.006

25. S. Askar, The rise of complex phenomena in Cournot duopoly games due to demand functions without inflection points, *Commun. Nonlinear Sci. Numer. Simul.*, **19** (2014), 1918–1925. https://doi.org/10.1016/j.cnsns.2013.10.012

26. N. Sirghi, M. NeamTu, P. C. Strain, Analysis of a dynamical cournot duopoly game with distributed time delay, *Timisoara J. Econ. Bus.*, **8** (2015), 1–13.

27. S. S. Askar, A. Al-khedhairi, Cournot duopoly games: Models and investigations, *Mathematics*, **7** (2019), 1079.

28. X. Yang, Y. Peng, Y. Xiao, X. Wu, Nonlinear dynamics of a duopoly stackelberg game with marginal costs, *Chaos, Solitons Fractals*, **123** (2019), 185–191. http://doi.org/10.1016/j.chaos.2019.04.007

29. Y. Peng, Y. Xiao, Q. Lu, X. Wu, Y. Zhao, Chaotic dynamics in cournot duopoly model with bounded rationality based on relative profit delegation maximization, *Phys. A: Stat. Mech. Appl.*, **560** (2020), 125174. https://doi.org/10.1016/j.physa.2020.125174

30. S. S. Askar, A. Al-khedhairi, On complex dynamic investigations of a piecewise smooth nonlinear duopoly game, *Chaos, Solitons Fractals*, **139** (2020), 110001. http://doi.org/10.1016/j.chaos.2020.110001

31. J. Long, H. Zhao, Stability of equilibrium prices in a dynamic duopoly bertrand game with asymmetric information and cluster spillovers, *Int. J. Bifurcation Chaos*, **31** (2021), 2150240.

32. L. Wei, H. Wang, J. Wang, J. Hou, Dynamics and stability analysis of a stackelberg mixed duopoly game with price competition in insurance market, *Discrete Dyn. Nat. Soc.*, **2021** (2021), 3985367.

33. S. Askar, On dynamic investigations of cournot duopoly game: When firms want to maximize their relative profits, *Symmetry*, **13** (2021), 2235.

34. M. El Amrani, H. Garmani, D. Ait Omar, M. Baslam, B. Minaoui, Analysis of the chaotic dynamics duopoly game of isps bounded rational, *Discrete Dyn. Nat. Soc.*, **2022** (2022), 6632993.

35. Y.-l. Zhu, W. Zhou, T. Chu, Analysis of complex dynamical behavior in a mixed duopoly model with heterogeneous goods, *Chaos, Solitons Fractals*, **159** (2022), 112153. https://doi.org/10.1016/j.chaos.2022.112153

36. A. M. Awad, S. S. Askar, A. A. Elsadany, Complex dynamics investigations of a mixed bertrand duopoly game: Synchronization and global analysis, *Nonlinear Dyn.*, **107** (2022), 3983–3999. http://doi.org/10.1007/s11071-021-07143-2

37. Y. Zhang, T. Zhang, C. Wang, Complex dynamics of Cournot-Bertrand duopoly game with peer-induced fairness and delay decision, *Discrete Contin. Dyn. Syst. B*, **28** (2023), 2544–2564.

38. J. Long, F. Wang, Equilibrium stability of dynamic duopoly cournot game under heterogeneous strategies, asymmetric information, and one-way r&d spillovers, *Nonlinear Eng.*, **12** (2023), 20220313.

39. Z. Wei, W. Tan, A. A. Elsadany, I. Moroz, Complexity and chaos control in a cournot duopoly model based on bounded rationality and relative profit maximization, *Nonlinear Dyn.*, **111** (2023), 17561–17589. http://doi.org/10.1007/s11071-023-08782-3

40. H. Meskine, M. S. Abdelouahab, R. Lozi, Nonlinear dynamic and chaos in a remanufacturing duopoly game with heterogeneous players and nonlinear inverse demand functions, *J. Differ. Equations Appl.*, **29** (2023), 1503–1515.

41. S. S. Askar, A. M. Alshamrani, Cournot–Bertrand duopoly model: Dynamic analysis based on a computed cost, *Complexity*, **2024** (2024), 5594918.

42. R. Ahmed, A. Khalid, S. Karam, Exploring complex dynamics in a stackelberg cournot duopoly game model, *Phys. Scr.*, **99** (2024), 115036. http://doi.org/10.1088/1402-4896/ad881b

43. R. Ahmed, M. Z. A. Qureshi, M. Abbas, N. Mumtaz, Bifurcation and chaos control in a heterogeneous cournot-bertrand duopoly game model, *Chaos, Solitons Fractals*, **190** (2025), 115757. http://doi.org/10.1016/j.chaos.2024.115757

44. M. Azioune, M. S. Abdelouahab, R. Lozi, Bifurcation analysis of a cournot triopoly game with bounded rationality and chaos control via the ogy method, *Int. J. Bifurcation Chaos*, **35** (2025), 2530019.

45. R. M. Corless, G. H. Gonnet, D. E. G. Hare, D. J. Jeffrey, D. E. Knuth, On the LambertW function, *Adv. Comput. Math.*, **5** (1996), 329–359.

46. Yu.A. Kuznetsov, *Elements of Applied Bifurcation Theory*, 3 Eds., New York: Springer-Verlag, 2004.

47. Yu. A. Kuznetsov, H. G. E. Meijer, *Numerical Bifurcation Analysis of Maps: From Theory to Software*, Cambridge University Press, 2019.

48. W. Govaerts, Yu. A. Kuznetsov, R. Khoshsiar Ghaziani, H. G. E. Meijer, *CL_MATCONTM: A toolbox for continuation and bifurcation of cycles of maps*, Report, Universiteit Gent, Belgium, and Utrecht University, The Netherlands, 2008. Available from: `https://www.academia.edu/54598277/Cl_MatContM_A_toolbox_for_continuation_and_bifurcation_of_cycles_of_maps`.

49. N. Neirynck, B. Al-Hdaibat, W. Govaerts, Yu. A. Kuznetsov, H. G. E. Meijer, Using MatcontM in the study of a nonlinear map in economics, *J. Phys.: Conf. Ser.*, **692** (2016), 012013.

AIMS Press